LIMBO
Limb and occultation measurement simulator

E. Kyrölä, J. Tamminen, L. Oikarinen, E. Sihvola, P. Verronen, and G. W. Leppelmeier

Finnish Meteorological Institute, Geophysical Research Division, P.O. Box 503, FIN-00101 Helsinki, Finland
e-mail: erkki.kyrola@fmi.fi, johanna.tamminen@fmi.fi, liisa.oikarinen@fmi.fi, elina.sihvola@helsinki.fi, pekka.verronen@fmi.fi, gilbert.leppelmeier@fmi.fi

ABSTRACT

In this paper we present the LIMBO-simulator, which is developed to simulate occultation and limb measurements of the Earth's atmosphere. The LIMBO-simulator can be used to simulate the geographical positions of the measurements, absorption and scattering in the atmosphere, and the instrumental effects. It also includes an inversion module, which makes it possible to perform an end-to-end system simulation of a satellite instrument and its ground segment.

1 INTRODUCTION

Many of the present and planned satellite remote sensing instruments are very complex and expensive. New measurement ideas and improvements for the old ones are continuously proposed. It is no wonder that there is a growing sense that every new instrument concept should be tested thoroughly before the instrument is being built. The same conclusion holds for the related ground segment.

Basically, there are two types of simulators available. The most complete simulators are the ones that simulate one specific instrument and they are used to fine tune the instrument and the data processing software. Because of these qualifications this kind of simulator will be available only after the overall instrument and data processing concept have been nearly agreed. A complete simulator is quite an expensive undertaking and its construction is therefore carefully supervised. In the GOMOS project a complete end-to-end simulator development was carried out by the ACRI company after ESA adopted GOMOS as an ESA developed instrument for the ENVISAT-1 satellite. It consists of two parts, GOSS and GOPR. The first mentioned performs the simulation of the measurement whereas the second one takes care of the ground segment simulation.

The second type of simulators are targeted to more explorative use. The main purpose of this kind of

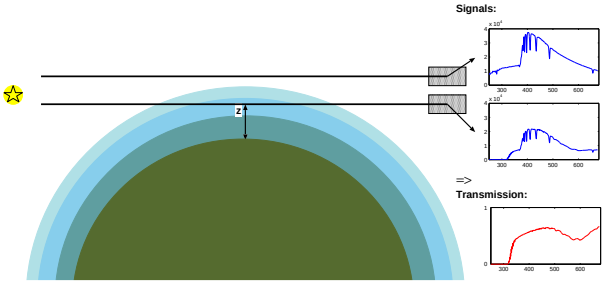

FIGURE 1. The principle of GOMOS stellar occultation measurement.

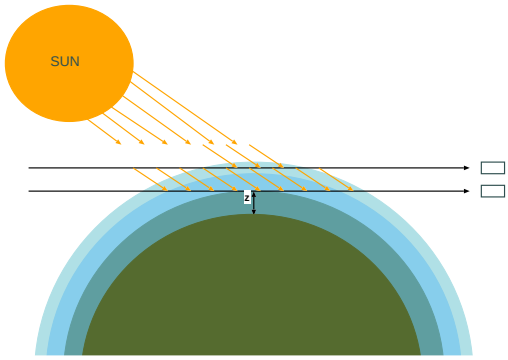

FIGURE 2. The principle of ODIN/OSIRIS limb measurement.

simulator is to assist in testing new instrument concepts and new data processing schemes. An example of such a simulator is LIMBO. It is developed to simulate the occultation measurements like the GOMOS (Fig. 1), and limb measurements like the ODIN/OSIRIS (Fig. 2). The measurement physics of occultation and limb measurements are discussed in Refs. 1–3.

LIMBO simulator is based on the FINGOM simulator, which was constructed at the Finnish Meteorological Institute (FMI) in order to help in design of the GOMOS instrument and to test and compare different data handling and inversion methods. It has been a valuable tool in guiding the instrument development of GOMOS and COALA (simplified version

of GOMOS). Moreover, it has formed a flexible platform for studying different data processing schemes for GOMOS. We also want to emphasize that the LIMBO-simulator have been an important assistance in Refs. 3–5.

In this paper the properties of the LIMBO-simulator are discussed and some examples of LIMBO products are given. We will restrict the discussion to the public version of LIMBO, which will be available during 1999 at Web site `http://www.geo.fmi.fi/AERON/LIMBO`. A more complete version of LIMBO is used at FMI but it includes features, which are more experimental and less documented.

2 STRUCTURE OF LIMBO

In general, the end-to-end data simulation can be divided into the following subtasks:

- measurement geolocation simulation
- simulation of emission, transmittance, and scattering in the atmosphere
- instrument simulation
- ground segment data processing simulation.

The LIMBO simulator is organized in a fully modular way (see Fig. 3). The data from one module to another is transferred in the form of ASCII-files. This gives the possibility to execute any single module independently. The individual modules are:

hocus	compute possible occultations
pocus	select occultations and compute measurement coordinates
starspec	compute stellar spectrum
refratra	compute ray tracing and transmission due to refraction including the scintillations
tarantella	compute transmission due to absorption and scattering, compute atmospheric radiance
instru	simulate instrument
noisead	compute noise from photon counting and model the instrument AD-conversion
inverse	perform spectral and vertical inversion

The programming language of LIMBO is FORTRAN 77 with some widely used F90 extensions like namelists for defining the input parameters.

The overall simulation is controlled by a general namelist. Additional lower level parameters to each module are provided by module namelists. The analysis and visualization of LIMBO results are supported by a collection of MATLAB-routines.

3 MEASUREMENT GEOLOCATION SIMULATION

To simulate the measurement geolocation we need to utilize the orbit simulator of the satellite where the instrument will be installed. Realistic orbit simulators are provided by satellite manufactures and space organizations.

In LIMBO the orbit simulation is strongly simplified. The shape of the earth is approximated by a sphere. The orbit is circular but the inclination and the time of the descending node of the solar-synchronous orbit can be defined by the user.

The instrument specific properties that need to be taken into account are the pointing targets of the instrument and the accessible field of view angles. For occultation instruments targets are stars, in some cases also planets, the Moon or the Sun. For the limb radiance measurement the target is the Sun illuminated limb, which is scanned in a predefined manner.

In occultation mode the geolocations are computed in two steps. First the module *hocus* calculates all the possible occultations. Next the module *pocus* selects an 'optimized' set of occultations and calculates the geolocational data, like the satellite position, field of view angle and the position of the Sun with respect to the field of view. Also some additional information like the stellar magnitude and temperature, start and end times, start and end latitude and longitude for the occultation are computed. An example of the output files is shown in Fig. 4.

In case of occultation measurements there is some freedom to make the mission planning optimization possible (see Ref. 4). At a given time there may be several star targets available and a decision must be made on which star the instrument should be pointed at. This selection depends on the mission objectives of the instrument because different stars provide varying information on the atmosphere. Such mission planning exercises have been carried out in the GOMOS project. A simplified tool has been included in the present LIMBO simulator. At present the user can select between three different optimization routines:

- selecting stars in time order
- favouring bright stars
- favouring polar occultations.

4 STELLAR AND SOLAR SPECTRA

The wavelength range of LIMBO covers ultraviolet and visible wavelengths. There are no measurements of stellar spectra covering the whole of this spectral region. The ground based measurements are limited by the small transmission of the Earth's atmosphere

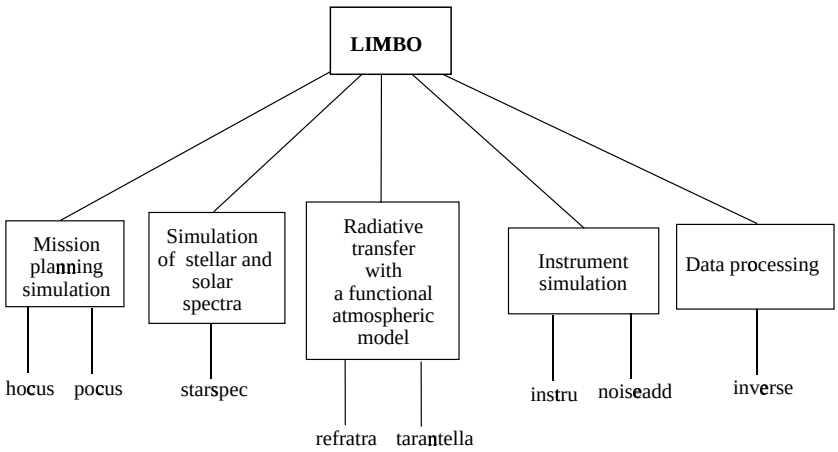

FIGURE 3. The modular structure of LIMBO simulator. Each one of the modules can be activated separately since the input parameters are transfered as ASCII-files.

% nro	time	star nro	sat rad	sat teta	sat phi	star teta	star phi	sun teta	sun phi	tan alt	tan teta	tan phi
1	97.00	53	7178.388	79.702	-124.574	-17.986	10.493	-11.48	-152.49	122.164	70.362	-14.017
136	103.00	53	7178.388	79.474	-126.428	-17.986	10.465	-11.48	-152.52	100.926	70.388	-13.868
141	104.00	53	7178.388	79.465	-126.495	-17.986	10.464	-11.48	-152.52	100.134	70.389	-13.862
161	105.00	53	7178.388	79.430	-126.762	-17.986	10.459	-11.48	-152.53	96.960	70.392	-13.840
181	106.00	53	7178.388	79.396	-127.028	-17.986	10.455	-11.48	-152.53	93.778	70.396	-13.818
201	107 00	53	7178 388	79 360	-127 292	-17 986	10 451	-11 48	-152 54	90 590	70 400	-13 796

%orbit: 1

%star nro	magn	temp	start time	occ time	move time	wait time	sc azi	tan1 lat	tan1 long	tan2 lat	tan2 long	suntan ele
53	2.04	4800.0	97.00	36.00	0.00	97.00	188.38	70.36	-14.02	70.50	-13.20	-64.39
6	0.08	5400.0	2033.00	72.00	37.57	1862.43	239.67	-12.81	147.08	-15.59	143.61	-73.27
46	1.98	4400.0	3846.50	46.50	22.80	1718.70	219.90	-52.55	24.40	-50.62	24.98	31.11
101	2.60	24000.0	4303.50	36.00	36.76	373.73	171.24	-39.28	-15.72	-39.28	-16.34	-41.54
66	2.21	4200.0	4414.00	39.00	29.13	45.37	205.34	-28.03	-1.65	-27.33	-0.84	79.30
93	2.50	24000.0	4524.50	36.50	17.28	54.22	195.28	-24.01	-7.86	-23.73	-7.38	38.88
71	2.25	7700.0	4585.00	36.50	13.35	10.65	192.88	-20.94	-9.90	-20.72	-9.52	-56.69
39	1.86	4400.0	4684.50	37.50	14.44	48.56	197.99	-14.25	-9.45	-13.90	-8.90	-40.44
119	2.70	4400.0	4776.00	52.00	25.99	28.01	226.30	-1.34	-1.63	0.66	-0.33	67.11
159	2.93	4700.0	4884.50	42.50	19.04	37.46	213.34	0.84	-6.85	1.82	-5.82	-36.60
2	-0.72	7400.0	4961.50	42.00	13.10	21.40	211.84	4.85	-8.30	5.74	-7.28	1.10
133	2.80	5800.0	5185.50	36.00	32.07	149.93	172.35	12.49	-26.87	12.47	-27.35	-7.18
106	2.64	15000.0	5298.00	61.50	42.89	33.61	233.99	30.41	-3.77	32.91	-1.46	-24.77
9	0.46	22000.0	5469.00	35.50	36.67	72.83	186.11	29.97	-24.74	30.03	-24.60	54.49
83	2.39	4900.0	5763.50	35.50	15.63	243.37	178.96	46.52	-33.79	46.51	-34.00	-39.68

FIGURE 4. An example of the input/output files of the mission planning simulation block. Upper table: measurement geolocation file. Lower table: additional information about the selected stars.

in the UV-region. Satellite measurements of stellar spectra are made only at UV-wavelengths. In the public version of LIMBO we provide the following possibilities to simulate the stellar spectra:

Blackbody spectra The blackbody spectrum is evaluated at the specified stellar temperature and it is normalized to the visual magnitude of the star. The blackbody spectrum is a simple model that ignores sharp characteristics of the spectrum.

Solar spectrum damped to stellar intensity values] The advantage of the solar spectrum is that it includes Fraunhofer lines and other realistic structures of real stellar spectrum.

User defined The user can define his/her own spectra, which is read from a file.

5 SIMULATION OF TRANSMISSION AND SCATTERING IN THE ATMOSPHERE

An important part of the simulation is the simulation of the atmospheric response. The structure of the atmosphere is, of course, central as the objective of the simulation is to explore what information a remote sensing measurement can provide of the atmospheric constituents.

The model is based as much as possible on functional description of the atmosphere. The advantage is that the model is very concise and therefore it is easy to check and modify. The model properties are listed in the following subsections.

5.1 Refraction

The first step in the transmission simulation is the tracing of the ray path in the atmosphere. Refraction bends the ray path light travels in the atmosphere

and therefore it affects also the absorption and scattering of stellar light. In stellar occultation measurements the refraction also causes directly attenuation of light intensity due to refractive dilution.

The ray tracing is accomplished by iteratively solving the differential equation describing the bending of the ray path in the atmosphere. In the occultation mode we know the satellite position and the stellar direction whereas the pointing angle of the instrument is unknown (it is known only when we actually make measurements).

The refractive attenuation from a point source can be calculated as

$$T_{ref}(z) = \frac{1}{1 + L\frac{d\alpha}{dz}}, \qquad (1)$$

where L is the distance from the satellite to the tangent point, z is the tangent altitude, and α is the refraction angle. The value for the refractive attenuation can only be calculated after a complete refraction calculation at all tangential altitudes. However, the attenuation can also be approximated by a closed formula. Both possibilities are included in the LIMBO simulator. The refractive attenuation, which is almost independent of wavelength, is most significant at low tangent altitudes where it can be as large as 0.5.

In addition to the refractive dilution we also simulate scintillations (see Ref. 1) by a random process.

5.2 Attenuation due to absorption and scattering

The attenuation of the light due to absorption and scattering can be evaluated by following the trajectory calculated by the ray tracing and using the densities and cross sections of different absorbers and scatterers. At each point along the trajectory the temperature values are also checked and appropriate temperature corrections for the cross sections are performed. The transmission is then

$$T_{abs} = e^{-\tau}, \qquad (2)$$

where the optical depth is given by

$$\tau(\lambda, \ell(\lambda)) = \sum_j \int \rho_j(s)\sigma_j(\lambda, \mathrm{T}(s))ds. \qquad (3)$$

The densities $\rho_j(s)$ and the cross sections $\sigma_j(\lambda, \mathrm{T}(s))$ of the constituents are discussed below.

5.3 Solar light scattering

The simulation of the solar scattering term starts by the calculation of the direction of the Sun with respect to the star-satellite line. If this line is in a full shadow no scattering term calculation will be performed. If not, a single scattering approximation calculation is carried out. The single scattering contribution is

$$I_{scatt}(\lambda) = I_{Sun}(\lambda) \times \int_{LOS} T_{Sun}(s,\lambda)T_{ext}(s,\lambda)K(s,\lambda)ds, \qquad (4)$$

where I_{Sun} is the solar irradiance. The transmissions T_{Sun} and T_{ext} and are connected to the paths from the Sun to the scattering point and from the scattering point to the satellite, respectively. The scattering kernel is

$$K(s,\lambda) = \rho_{air}P_R(\theta)\sigma_R(\lambda) + \rho_a P_a(\theta)\sigma_a(\lambda), \qquad (5)$$

where the cross sections σ_R and σ_a are the Rayleigh and aerosol scattering cross sections and P_R and P_a are the corresponding phase functions. The phase function for aerosol scattering is taken to be the Henyey-Greenstein function (see e.g. Ref. 6). The angle θ is the scattering angle.

The multiple scattering calculations have not been included in LIMBO (see Ref. 2).

Besides the stellar signal and the scattering term other radiation sources may also be of importance. At least the atmospheric UV and optical emissions, auroral emissions and thermal emissions can be identified. Thermal emissions can be ignored in the wavelength region of LIMBO. The auroral and UV-optical emissions will contribute to the signals of limb measurements. Presently they are not simulated by LIMBO.

5.4 Atmospheric model

The atmospheric model is based on a functional modeling of the atmosphere instead of tables usually exploited. Most of the modeling has been built on three different stages of complexity (model types) in the following way:

Type 0: Simple model with a fast execution time

Type 1: Standard model. Only vertical variation. US Standard followed in temperature. Ozone distribution imitates the tables found in US Standard and in LOWTRAN. Other trace gases extracted from literature.

Type 2: Global, time-dependent model with latitudinal variations.

The atmospheric model includes temperature, neutral density, O_3, NO_2, NO_3, OClO, various aerosol models. The user can select for each of these variables the desired model type separately. An example of the complexity of the global, time-dependent modeling is given in Fig. 5.

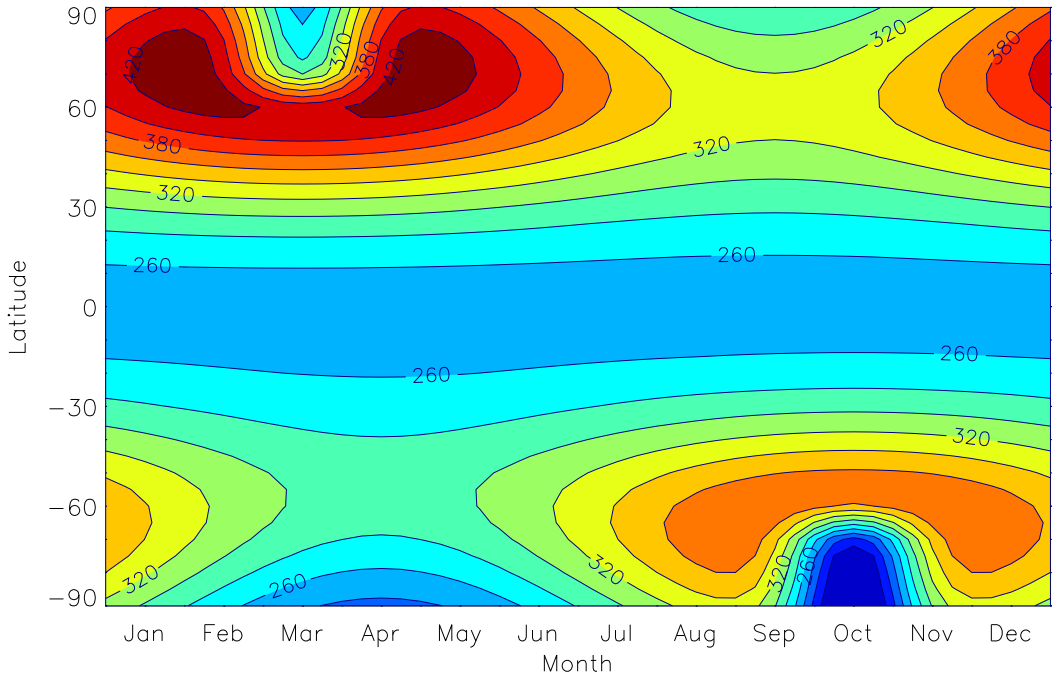

FIGURE 5. Total ozone column density as a function of month and latitude. The values correspond to ozone density model type 2 in LIMBO.

FIGURE 6. Transmission as a function of wavelength and tangent altitude

5.5 Absorption and scattering cross sections

The absorption cross sections of the gases are used as tables located in the supporting database. There certainly are some differences between values given by different experimenters but for our simulation purposes the differences are not relevant if we only use consistent data sets. Besides, the user can easily replace a given cross section by a new one.

Some cross sections are temperature dependent. We have available temperature dependence of O_3 and NO_2 in the form of cross sections measured at few different temperatures. The temperature dependence makes the cross sections dependent on the altitude (or more generally on position). To include the temperature dependence of O_3 and NO_2 we have used simple linear interpolation from the measured values.

The determination of the aerosol scattering cross section is difficult because aerosol distributions vary considerably. We have used the simple Ångström formula

$$\sigma(\lambda) = \sigma_0 \frac{1}{\lambda}, \tag{6}$$

where λ is the wavelength and σ_0 the scaling factor. Another possibility is to use user specified cross sections, which are read from a file.

6 INSTRUMENT SIMULATION

The instrument block simulates the instrumental transmission and gain the imaging properties of the instrument. The instrument simulation in LIMBO assumes that the detection device is CCD as in GOMOS and OSIRIS. The front end optics of the instrument form an image on the focal plane where also a slit is placed. The slit is taken here in the vertical direction with respect to the the limb. From that plane the image is imaged through a grating to a two dimensional CCD.

In the slit plane (u,v-plane) the source consists of the image of a star and a background. The number of electrons generated in one pixel can be written as

$$N(x,y,\Delta t) = \iiiiii dx\, dy\, du\, dv\, dt\, d\lambda \; Q(x,y,\lambda) h(x,y,u,v,\lambda) I(u,v,\lambda,t), \tag{7}$$

where Q is the quantum efficiency function of the CCD, h the point spread function and I the intensity in the slit plane. The integration is performed over one pixel in the CCD plane (dx, dy), over the slit plane (du, dv), over the wavelength region $(d\lambda)$ and over the measurement time (dt).

In order to build the instrument simulation we make use of several simplifications. For simplicity we show here only the star induced response.

The first simplification assumes a star to be a point in the slit plane. We further assume that the quantum efficiency is a smooth function of its variables and the impulse spread function is separable to x and y directions.. By binning in vertical direction over some interval we can write

$$N(x,\Delta t) = \iint dt\, d\lambda' I_{star}(\lambda', t) W(x, \lambda', t), \tag{8}$$

where W is the effective time-dependent instrument function. This formulation is the signal simulation simplification LIMBO uses.

The number of electrons simulated by Eq. (8) is a random process. The photo–electron counting probability follows the Poisson statistics. In addition of the Poisson noise we have noise generated by the instrument itself and the readout procedures. The dark current is actually an addition to the electron generation by photons. Therefore we include the dark current by adding the equivalent term in the detected number of electrons. After taking care of all these noise sources we amplify the signal and perform the A/D-conversion, which also adds some noise to the final result.

7 INVERSION MODULE

The inversion module provides simple inversion solutions for the occultation measurements. The limb scattering inversion will be provided later on.

The inversion module starts by some a few instrument-type corrections for the signals. The most important one is the subtraction of the estimated dark current form the signals. After this operation we can create the transmission function by dividing the stellar spectrum measured through the atmosphere with the reference spectrum:

$$T_{tot} = \frac{N}{N_{ref}} \tag{9}$$

This transmission includes in addition to the transmission due to molecular absorption and scattering also transmission modulation by the refractive dilution and by scintillations in the occultation mode.

Next we enter to the so-called Level 2. In the first step the modulations by refraction are removed and we arrive at the transmission function, which can be related to absorption and scattering effects only. An example of the simulated transmission can be found in the Fig. 6.

The spectral inversion is carried out by applying the Levenberg-Marquard solver for the transmission function. The vertical inversion is based on the simple onion peeling method. In Fig. 7 we present retrieved NO_2 profile with estimated 2σ error bars. An example of the retrieved ozone density accuracies are shown in Ref. 4 .

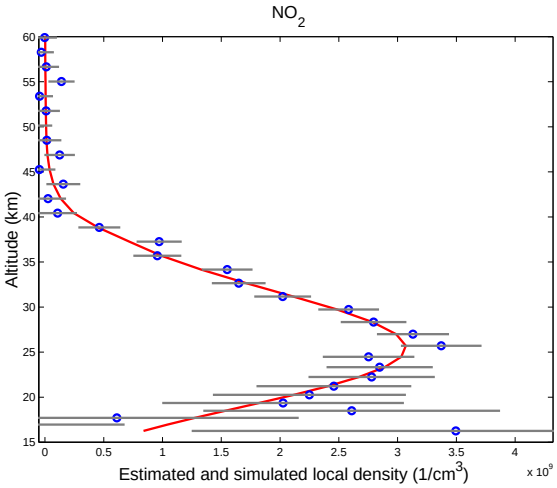

FIGURE 7. Retrieved NO_2 profile with 2σ-error bars and the 'true' profile used in forward simulation (solid line)

8 DISCUSSION

The presented LIMBO simulator contains many years of work and development in different areas of limb-measuremnts of the atmosphere. The LIMBO simulator is a quite versatile end-to-end simulator for limb-measurements. The code is very flexible. Different combinations of the simulation tasks can be activated separately. New characteristics can easily be added to the present version. The LIMBO simulator makes also statistical studies of the ground processing schemes possible.

REFERENCES

1. E. Kyrölä. GOMOS ATBD - Level 2. In this volume, 1999.
2. L. Oikarinen. Monte Carlo simulations of radiative transfer for limb scan measurements. In this volume, 1999.
3. H. Auvinen, L. Oikarinen, E. Kyrölä, J. Tamminen, and G. W. Leppelmeier. Inversion algorithms for OSIRIS and GOMOS bright-limb background term. In this volume, 1999.
4. E. Kyrölä and J. Tamminen. GOMOS mission planning. In this volume, 1999.
5. J. Tamminen, E. Kyrölä, and H. Auvinen. MCMC algorithms for inverse problems in remote sensing. In this volume, 1999.
6. K.N. Liou. *Radiation and Cloud Processes in the Atmoshpere*. Oxford University press, 1992.